Wuhan University
Journal of Natural Sciences

2013, Vol.18 No.2, 133-141

Article ID 1007-1202(2013)02-0133-09
DOI 10.1007/s11859-013-0905-0

Molecular Dynamics Simulation of RNA Pseudoknot Unfolding Pathway

☐ **GUO Yun, ZHANG Wenbing†**

School of Physics and Technology, Wuhan University, Wuhan 430072, Hubei, China

Abstract: Many biological functions of RNA molecules are related to their pseudoknot structures. It is significant for predicting the structure and function of RNA that learning about the stability and the process of RNA pseudoknot folding and unfolding. The structural features of mouse mammary tumor virus (MMTV) RNA pseudoknot in different ion concentration, the unfolding process of the RNA pseudoknot, and the two hairpin helices that constitute the RNA pseudoknot were studied with all atom molecule dynamics simulation method in this paper. We found that the higher cation concentration can cause structure of the RNA molecules more stable, and ions played an indispensable role in keeping the structure of RNA molecules stable; the unfolding process of hairpin structure was corresponding to the antiprocess of its folding process. The main pathway of pseudoknot unfolding was that the inner base pair opened first, and then, the two helices, which formed the RNA pseudoknot opened decussately, while the folding pathway of the RNA pseudoknot was a helix folding after formation of the other helix. Therefore, the unfolding process of RNA pseudoknot is different from the antiprocess of its folding process, and the unfolding process of each helix in the RNA pseudoknot is similar to the hairpin structure's unfolding process, which means that both are the unzipping process.

Key words: RNA pseudoknot; molecular dynamics simulation; stability; unfolding; pathway
CLC number: O 469; Q 61

Received date: 2012-06-26
Foundation item: Supported by the National Natural Science Foundation of China (10774115) and the Doctoral Fund of Ministry of Education of China (20110141110009)
Biography: GUO Yun, female, Master candidate, research direction: RNA molecular dynamics. E-mail: guoyun@whu.edu.cn
† To whom correspondence should be addressed. E-mail: wbzhang@ whu.edu.cn

0 Introduction

RNA is a kind of important biological macromolecules. The biological functions of RNA are very complex and rich, covering almost all aspects of gene's storage, replication, expression, and regulation[1,2]. To realize these functions, the chain-like RNA molecules often form a more complex structure through the processes of pairing, shrinkling, and folding[3,4].

Many biological functions of RNA are related to their pseudoknot structures[5-15]. For instance, the psuedoknot in the central of catalytic domain forms the core structure motif in the telomerase RNA[16-18]. Moreover, many viruses regulate retroviral gene expression by ribosomal frameshifting, while the pseudoknot plays an indispensable role in promoting ribosomal frameshifting[19-28]. In addition, the pseudoknot mutation, which is caused by strengthening or weakening it stability thermally or mechanically, can lead to the change of ribosomal frameshifting efficiency[29,30]. For these and other problems of RNA, it is essential to reveal the mechanism of RNA function and design therapeutic strategies for the diseases in order to quantitatively predict the structure and stability of pseudoknot. The structural feature of pseudoknot provide a very favorable model to further study the folding and unfolding of complex biological molecules. Some excellent works about RNA pseudoknot have been studied, such as the folding/unfolding process of a pseudoknot in human telomerase RNA was researched using optical tweezers at different loads[31,32], which give direct evidence of the formation of nonnative structures and complex folding pathways. However, the folding/unfolding pathways for other RNA pseudoknots

and how the pathways would change under different conditions are still not clear.

Mouse mammary tumor virus (MMTV) is a complex retrovirus that uses the host immune system, which can insert the gene into the host chromosome and keep hibernation in the breast cells for many years[33-36]. Moreover, MMTV will be active again when the female rats become sexual maturity and pregnancy. Previous studies[33-36] have shown that over 90% incidences of the mouse breast cancer are related to the MMTV. In this paper, the unfolding process of MMTV RNA molecule (protein data bank (PDB) ID: 1KPD) is studied with all atom molecule dynamics simulation methods, from which we can obtain structure transition at the atomistic scale. To study the factors that affect the stability and the unfolding pathways of the pseudoknots, the MMTV RNA was studied by all-atom molecule dynamics simulation methods under different ion concentrations and temperatures.

1 Methods

In this paper, all simulations were performed using NAMD[37] molecule dynamics simulation software, which is considered as one of the best and has been widely applied to the simulation of biological macromolecules, such as RNA[38-40] and others, with CHARMM27 all atom force field[41-43]. The TIP3P water model is adopted, and Na ions are added to maintain the whole system's electrical neutrality. Using periodic boundary conditions, a rectangular water box is established as the distance between the box boundary and the atoms of the RNA molecule in the box is at least 25 Å. The long-range electrostatic interactions are calculated by the particle mesh Ewald method. The system uses isothermal isobaric ensemble, and the time step is set as 1 fs.

The initial structures are obtained from the protein data bank (PDB). These structures may contain extremely distorted, stretched, or deformed bonds and angles. Therefore, the structures need to be further optimized to obtain a most stable and minimum energy structure. Simulations first run 5 000 steps for the energy minimization of the entire RNA-aqueous solution and then run different steps of molecular dynamics to make the system equilibrium at certain temperature.

The secondary structure and tertiary structure of MMTV are showed in Fig. 1. The pseudoknot has 32 nucleotides (nt) and is constituted by two double helices (helix 1 and helix 2). The two helices stack coaxially on each other and form a long quasi-continuous helix in space. The pseudoknot is denoted by five parts: stem1, stem 2, loop 1, loop 2, and loop 3 (see Fig.1(b)). Stem 1 contains 5 base pairs, loop 1 contains 3 unpaired nucleotides, while stem 2 contains 4 base pairs, loop 2 contains 8 unpaired nucleotides, loop 3 contains two unpaired nucleotides.

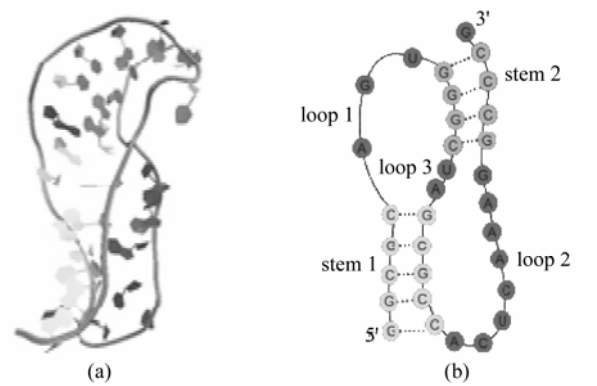

Fig. 1 Three-dimensional structure (a) and tertiary structure (b) of MMTV

RNA structure is characterized by the formation of base pairs, and the criterion of forming a base pair is the relevant atoms forming hydrogen bonds. If the bond and angle are in the specified range (bond length$\leqslant$3.5 Å, bond angle$\geqslant$120°), the base pair is formed. For base pair G—C, the three pairs of atoms which form hydrogen bond are G (O6)—C (N4), G (N1)—C (N3), and G (N2)—C (O2); and for AU base pair, they are A (N6)—U (O4) and A (N1)—U (N3).

2 Results and Discussion

2.1 Effects of Ion Concentration on the Structure of RNA Pseudoknot

Each phosphate group in the main chain of RNA molecules has a unit of negative charge, so there is a strong electrostatic repulsion between the main chains due to the strong negative charges of the main chain. If the RNA will form a stable structure, it should be in the salt solution, in which the metal ions are critical for RNA tertiary structural formation because the ions can neutralize backbone charge repulsion[44-46]. To study the effects of the ion concentration on the structure of RNA, the pseudoknot structures were studied in the NaCl solution with two ion concentrations 0.1 mol/L and 0.5 mol/L at the same temperature (290 K) and same pressure (1atm); meanwhile, 32 Na^+ ions were mingled within water in order to make the total charge of the RNA become zero. The hydrogen bonds of the two heli-

ces of the RNA pseudoknot during the simulation time at the two ion concentrations of 0.5 mol/L and 0.1 mol/L are shown in Figs. 2 and 3, respectively. It shows that at the concentration of 0.5 mol/L, all the hydrogen bond lengths of the base pairs are within the range of 3.5 Å and keep stable, while at the concentration of 0.1 mol/L, the hydrogen bond of the base pairs are not quite stable.

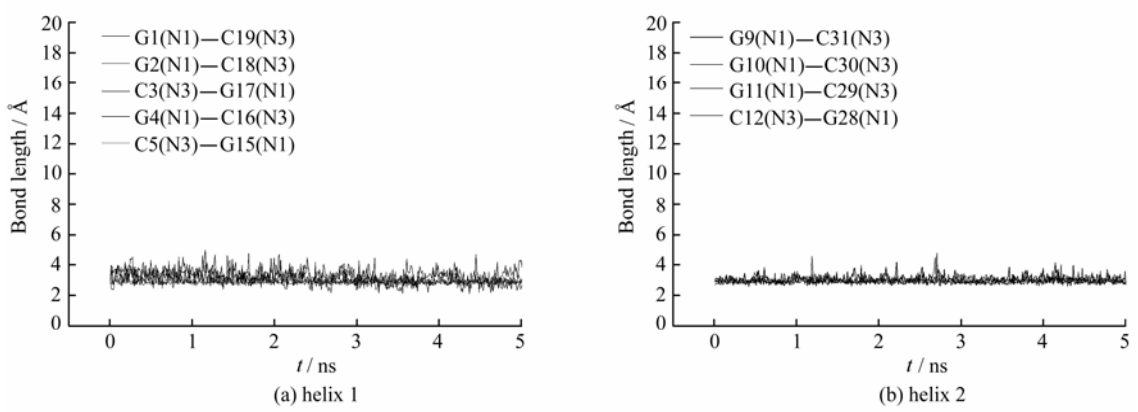

Fig. 2 Distribution of hydrogen bond at the concentration of 0.5 mol/L

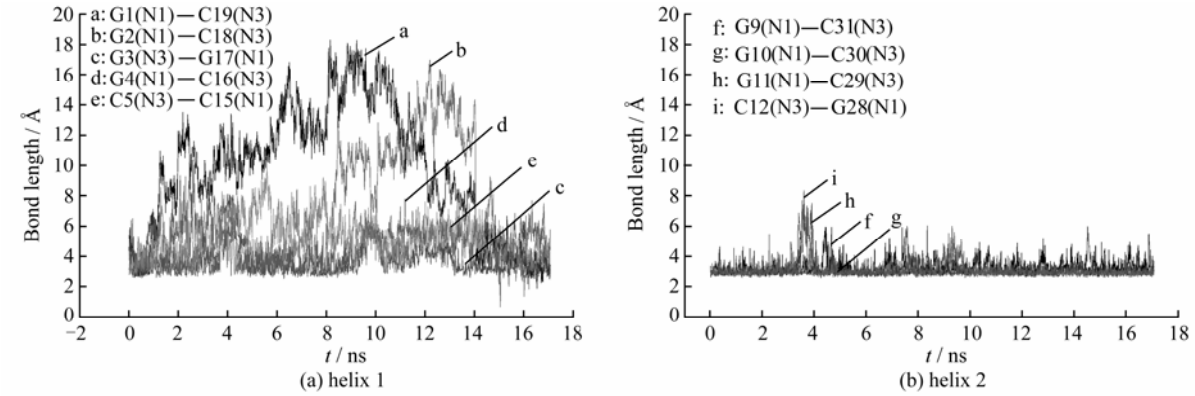

Fig. 3 Distribution of hydrogen bond at the concentration of 0.1 mol/L

The above results indicate that the ions played an indispensable role in keeping the structure stable for RNA molecules, the higher cation concentration will cause the more stable structure of the RNA molecules. As the main chain of RNA has strong negative charge, forming the base pair between different nucleotides must overcome the strong electrostatic repulsion between the main chains. The positive ions in the salt solution could neutralize the negative charge of the RNA, and the higher ion concentration makes it easier to form a compact structure.

2.2 Unfolding Process of RNA Pseudoknot

The free energy of pseudoknot[47] can be calculated by

$$G = G_{\text{stem}} + G_{\text{loop}} \tag{1}$$

where G_{stem} is the free energy of the two helices, which can be calculated by the nearest neighbor model, $G_{\text{stem}} = \sum G_{\text{stack}}$, and G_{stack} is the free energy[48-51] of a base stacking. G_{loop} is the free energy of the loops of the pseudoknot, which can be approximated as follows:

$$G_{\text{loop}} = 0.83 \times G_{\text{secondary}} + 0.2n_{\text{f}} + 0.1n_{\text{p}} \tag{2}$$

where $G_{\text{secondary}}$ is the sum of the free energies of the loop that are formed by the pseudoknot performed as secondary structure containing only helix 1 or helix 2; n_{f} is the number of unpaired nucleotide (14 nt); and n_{p} is the number of paired nucleotides (18 nt). The melting temperature T_{m} of the pseudoknot can be approximated as $T_{\text{m}} = \Delta H / \Delta S$, which is about 360 K[52].

The unfolding process of MMTV RNA pseudoknot is studied at the temperature of 400 K and 450 K in 0.5 mol/L NaCl solution. At these temperatures, the unfolding process can be achieved within a short time.

Figure 4(a) shows the probability of the paired bases accounting for the total number of paired bases of the native structure (base pairs retaining probability) during unfolding process at 400 K. It can be found that the base pairs retaining probabilities of helix 1 and helix

2 are all oscillating decreasing, which indicates that helix 1 and helix 2 are unfolding at the same time. The two helices unfold entirely in about 20 ns.

Figure 4(b) displays some important structures during the unfolding process of MMTV molecule in the temperature of 400 K. At 0.5 ns, the base pair 5C-15G of helix 1 is opened; at 6.5 ns, the 12C-28G base pair of helix 2 is opened; at 8.0 ns, the base pairs 5C-15G, 4G-16C of helix 1 and 12C-28G of helix 2 are opened; at 10.8 ns, 1G-19C of helix 1 is opened; and at 12.2 ns, 2C-18G is opened. Then, the base pairs 9G-31C, 10G-30C, and 11G-29C of helix 2 are opened in turn. The total base pairs of this RNA molecule are opened at 22.5 ns.

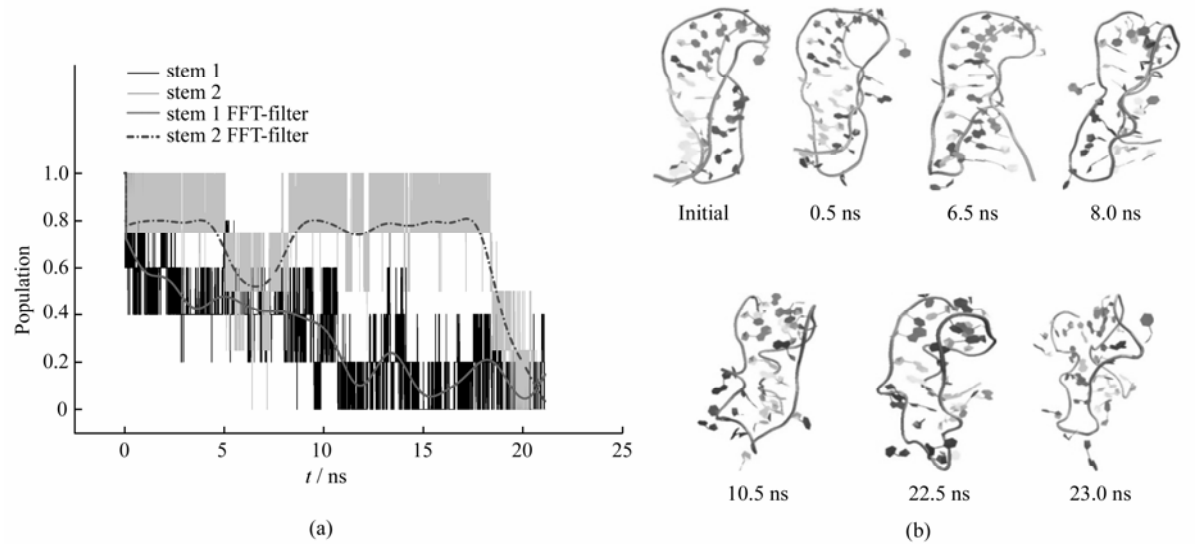

Fig. 4 MMTV RNA pseudoknot at 400 K

(a) Base pairs retaining probability of helix 1 and helix 2. The black curve characterizes the base pairs retaining population of helix 1, and the black bold curve is its fast Fourier transform filter (FFT-filter) curve. The light gray curve characterizes the base pairs retaining population of helix 2, and the grey dashed curve is its fast Fourier transform filter curve. (b) Some structural changes during the unfolding process.

Figure 5(a) indicates that the base pairs retaining probability during unfolding process at 450 K. As can be seen from the figure, helix 1 and helix 2 are unfolding almost at the same time, and the two helices that formed the RNA pseudoknot open decussately. At 1.5 ns, the base pair retaining the probability of helix 2 decreases to 0.5, while that of helix 1 decreases to 0.6. At 2.5 ns, the base pairs of helix 1 and helix 2 are totally opened, and the whole RNA molecule is unfolded.

Figure 5(b) shows some important intermediate structures during the unfolding process of MMTV molecule in the temperature of 450 K. At 0.5 ns, the base pair 5C-15G of helix 1 opens first, which make the pseudoknot form a bulge. At 1.5 ns, the opened base pairs include 5C-15G, 9G-31C, and 11G-29C; helix 1 and helix 2 are nearly opened at 2.5 ns, but the main chain conformation of the RNA molecule does not show enormous changes during the period. As the bases swing or reverse, base pairs show the characteristics of open-close switching. To 6.5 ns, the base pairs are all opened and RNA main chain would branch out, the structure of the RNA becomes loose gradually, and the entire RNA molecule transforms into a complete long chain.

From the above simulation results, we can find that the basic unfolding path of the pseudoknot at 400 K is similar to that at 450 K; the innermost base pair 5C-15G opens first, which is not difficult to understand, for the formation of this base pair results in structure distortions due to its innermost location, rendering the maximum entropy increase. The entropy change is about 37.08 cal/(K • mol) when the 5C-15G base pair is opened, which is greater than the entropy change of opening a single base pair. Next, the base pairs of the two helices open decussately, while RNA pseudoknot folding path was a helix folding after formation of the other helix. Therefore, the unfolding process of RNA pseudoknot differed from the antiprocess of its folding process. The unfolding process of each helix is an unzipping process and begins with each end of the helix.

2.3 Unfolding Processes of RNA Pseudoknot's Two Helices

To study the similarities and differences of the unfolding process of the pseudoknot molecule and isolate hairpin molecule, we simulated the unfolding process of the two helices (Fig. 6), which constitute the RNA

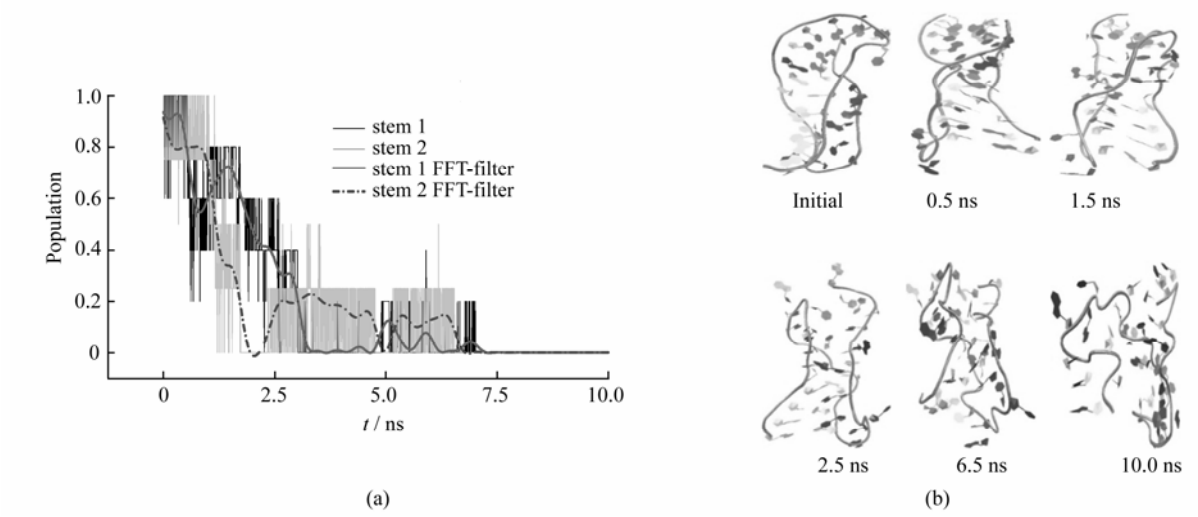

Fig. 5 MMTV RNA pseudoknot at 450 K

(a) The base pairs retaining population of helix 1 and helix 2 over time, The black curve characterizes the base pairs retaining population of helix 1, and the black bold curve is its fast Fourier transform filter (FFT-filter) curve. The light gray curve characterizes the base pairs retaining population of helix 2, and the gray dashed curve (dashed line) is its fast Fourier transform filter curve. (b) Some structural changes during the unfolding process

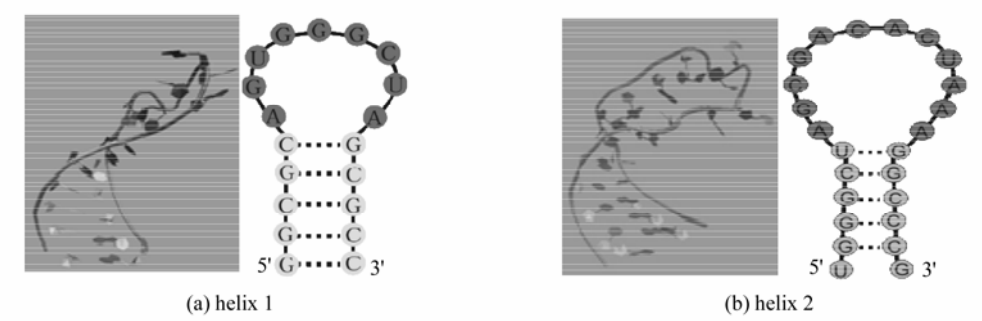

Fig. 6 Three-dimensional structure and secondary structure of the helices

pseudoknot in 0.5 mol/L NaCl solution at 400 K and 450 K, respectively. From the nearest neighbor model, the entropy and enthalpy of helix 1 are –164.4 cal/(K • mol) and –58.9 kcal/mol, respectively. The melting temperature is 358 K. For helix 2, the entropy and enthalpy are –190.5 cal/(K• mol) and –67.5 kcal/mol, respectively. The melting temperature is 354 K. The two melting temperatures are similar with that of the pseudoknot molecule.

Figure 7(a) displays the base pairs retaining probability of helix 1 during unfolding process at 400 K. We find that the base pairs of helix 1 completely open in about 3 ns. Figure 7(b) shows some important structures during the unfolding process. At 0.55 ns, the base pairs of 1G-19C, 2C-18G at the end of the helix open in turn; at 1.6 ns, the base pair 5C-15G near the loop opens; to 2.0 ns, 3C-17G opens; at 2.4 ns, the last remaining paired base pair 4G-16C opens, and then, the entire helix of the hairpin completely opens in less than 3.0 ns.

Figure 8(a) shows the base pairs retaining probability of helix 1 during unfolding process at 450 K, which indicates that the base pairs of helix 1 completely open in about 2.5 ns. Figure 8(b) shows some important structures during the unfolding process. At 0.5 ns, the base pair of 1G-19C in the end of the helix opens, followed by the opening of 2C-18G base pair at 0.6 ns, then at 1.0 ns, the base pair 5C-15G near the loop opens, at 1.6 ns, 4G-16C opens, and at 1.7 ns, the last base pair 3C-17G opens. Thus, the RNA is unfolded completely.

Figure 9(a) shows the base pairs retaining probability of helix 2 during unfolding process at 400 K. The base pairs of helix 2 are completely open in about 5 ns as the figure shows. Figure 9(b) displays some representative structures during the unfolding process of helix 2. The base pair 2G-24C at the end of helix 2 opens first at 2.2 ns, and at 2.8 ns, the base pair 6U-20G near the loop opens, when it is at 3.4 ns, 4G-22C opens, the base pair 5C-21G opens at 4.4 ns. The unfolding process of helix 2 is an unzipping process, which begins with the two ends of the helix.

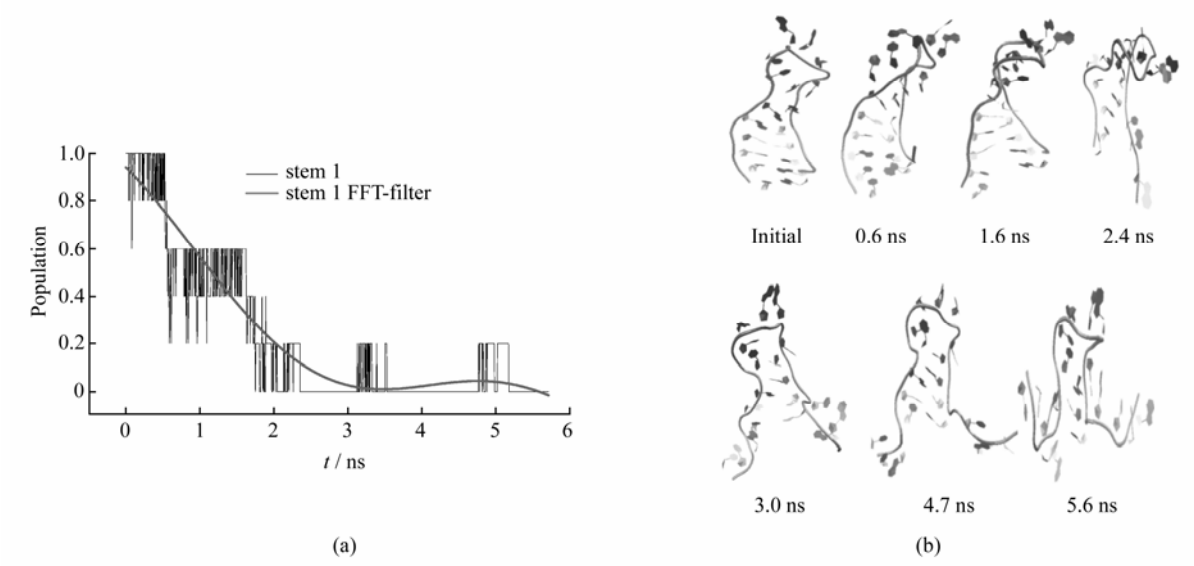

Fig. 7 Helix 1 at 400 K

(a) Relationship of base pair retaining population over time; (b) Some important intermediate structures during the unfolding process

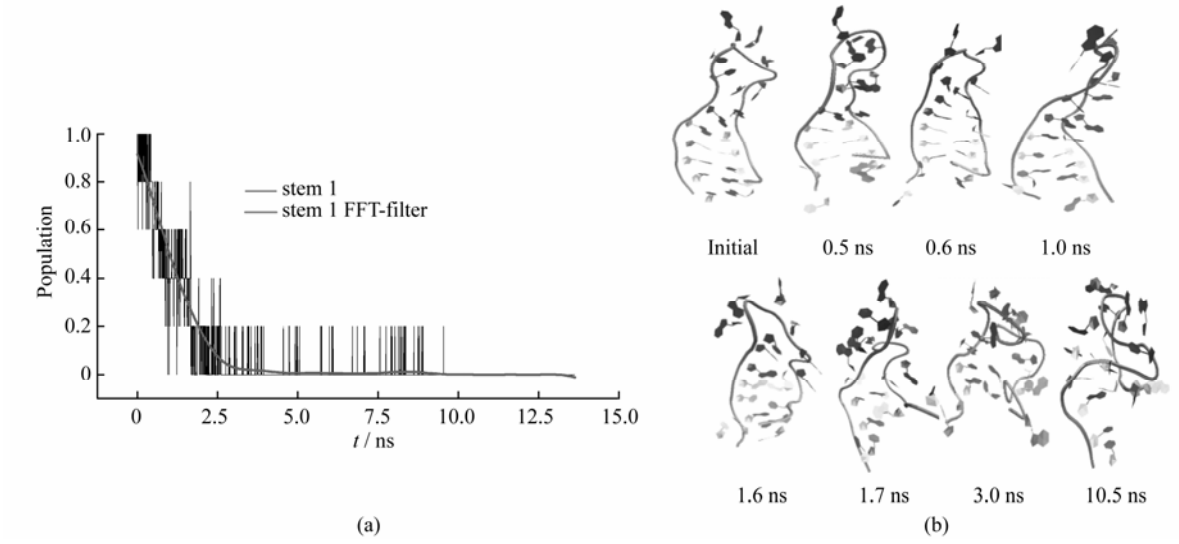

Fig. 8 Helix 1 at 450 K

(a) Relationship of base pair retaining population over time; (b) Some important intermediate structures during the unfolding process

Figure 10(a) indicates the base pairs retaining probability of helix 2 during unfolding process at 450 K, which indicate that the base pairs of helix 2 are completely open in about 1.5 ns. Figure 10(b) displays some representative structures during the unfolding process of helix 2. The base pair 6U-20G, which is near the loop, opens first at 0.7 ns, then 5C-21G follows at 0.9ns, at 1.2 ns, 2G-24C opens, and after the opening of 4G-22C at 1.5 ns, the whole RNA is full opened.

Comparing the unfolding process of the RNA pseudoknot and its two constituent hairpin helices, it can be seen that the unfolding process of RNA is a complex process, and the unfolding process of a pseudoknot is different from that of a hairpin structure. The main unfolding path of a hairpin structure is given as follows: the base pair at the two ends of the helix opens first, and then it is unfolded by an unzipping process. The unfolding process is corresponding to the antiprocess of its folding process. While RNA pseudoknot folding path was a helix folding after formation of the other helix, the unfolding process of RNA pseudoknot differed from the antiprocess of the folding process. The unfolding process of each helix in the RNA pseudoknot is similar to the hairpin structure's unfolding process, and both are the unzipping process.

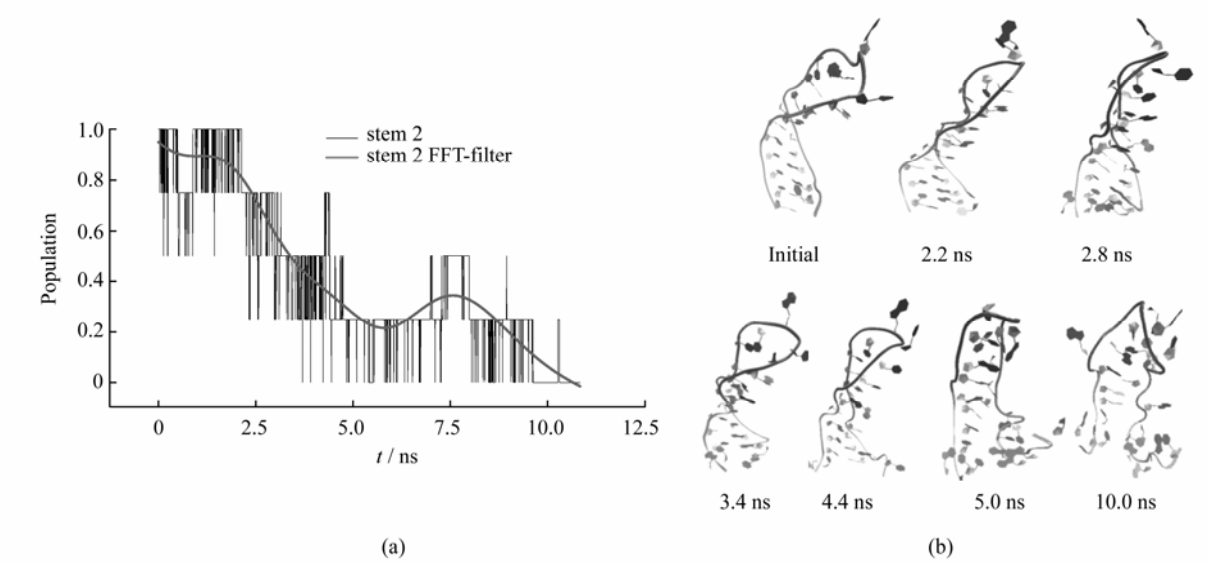

Fig. 9 Helix 2 at 400 K

(a) Base pair retaining probability during unfolding; (b) Some important intermediate structures during the unfolding process

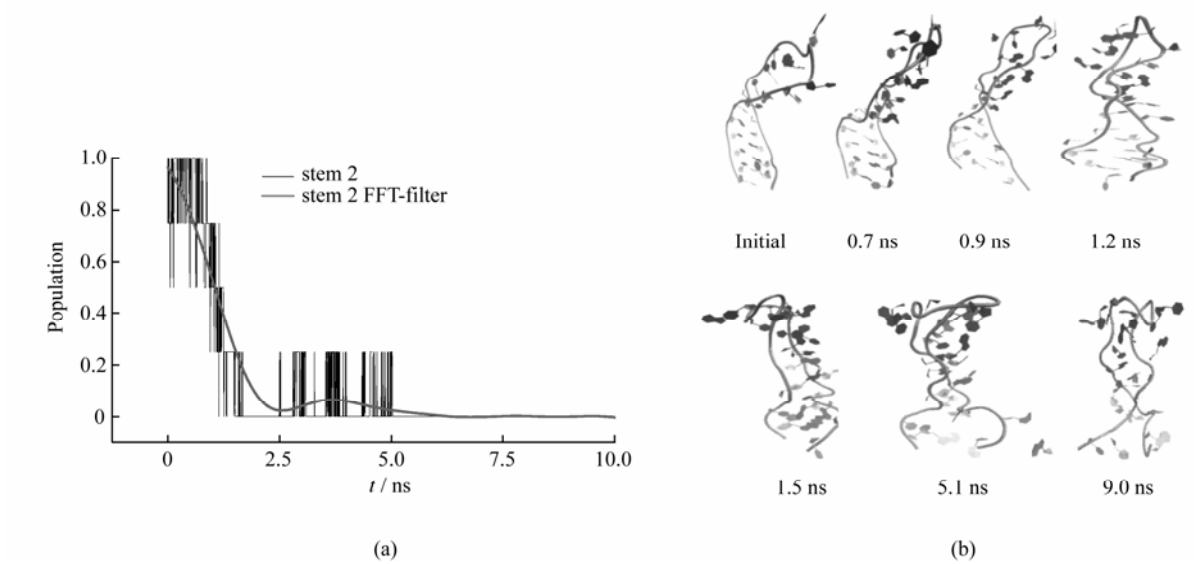

Fig. 10 Helix 2 at 450 K

(a) Base pair retaining probability during unfolding; (b) Some important intermediate structures during the unfolding process

3 Conclusion

The structural features of MMTV RNA pseudoknot in different ion concentration, the unfolding process of RNA pseudoknot, and two hairpin helices that constituted the RNA pseudoknot were studied with all atom molecular dynamics simulation method in this paper. We found that the higher cation concentration can cause more stable the structure of the RNA molecules and that the unfolding process of hairpin structure was corresponding to the antiprocess of its folding process. The main path of pseudoknot unfolding was that the inner base pair opened first, and then, the two helices that formed the RNA pseudoknot opened decussately. The unfolding process of RNA pseudoknot is different from the ant-process of its folding process. The unfolding process of each helix in the RNA pseudoknot was similar to the hairpin structure's unfolding process; both were the unzipping processes.

References

[1] Mattick J S, Igor V, Makunin I V. Non-coding RNA [J]. *Human Molecular Genetics*, 2006, **15**: 17-29.

[2] Kampa D, Cheng J, Kapranov P, *et al*. Novel RNAs identified from an in-depth analysis of the transcriptome of

human chromosomes 21 and 22 [J]. *Genome Res*, 2004, **14**(3): 331-342.

[3] Chen Shijie, Tan Zhijie, Cao Song, *et al*. The statistical mechanics of RNA folding [J]. *Physics*, 2006, **35**(3): 218-229(Ch).

[4] Zhao P N, Zhang W B, Chen S J. Predicting secondary structural folding kinetics for nucleic acid [J]. *Biophysical Journal*, 2010, **98**: 1617-1625.

[5] Sosnick T R, Pan T. RNA folding: Models and perspectives [J]. *Current Opinion in Structural Biology*, 2003, **13**(3): 309-316.

[6] Treiber D K, Williamson J R. Exposing the kinetic traps in RNA folding [J]. *Current Opinion in Structural Biology*, 1999, **9**(3): 339-345.

[7] Cao S, Giedroc D P, Chen S J. Predicting loop-helix tertiary structural contacts in RNA pseudoknots [J]. *RNA*, 2010, **16**: 538-552.

[8] Cao S, Chen S J. Biphasic folding kinetics of RNA pseudoknots and telomerase RNA activity [J]. *Journal of Molecular Biology*, 2007, **367**: 909-924.

[9] Cao S, Chen S J. Predicting structures and stabilities for H-type pseudoknots with interhelix loops [J]. *RNA*, 2009, **15**: 696-706.

[10] Zhang Y J, Zhang J, Wang W. Atomistic analysis of pseudoknotted RNA unfolding [J]. *Journal of the American Chemical Society*, 2011, **133**(18): 6882-6885.

[11] Thirumalai D, Hyeon C. RNA and protein folding: common themes and variations [J]. *Biochemistry*, 2005, **44**(13): 4957-4970.

[12] Woodson S A. Structure and assembly of group I introns [J]. *Current Opinion in Structural Biology*, 2005, **15**(3): 324-330.

[13] Lee T S, Giambasu G M, Harris M E, *et al*. Characterization of the structure and dynamics of the HDV ribozyme in different stages along the reaction path [J]. *The Journal of Physical Chemistry Letters*, 2011, **2**: 2538-2543.

[14] Chen S J. RNA folding, conformational statistics, folding kinetics, and ion electrostatics [J]. *Annual Review of Biophysics*, 2008, **37**: 197-214.

[15] Tinoco I Jr, Bustamante C. How RNA folds [J]. *Journal of Molecular Biology*, 1999, **293**: 271-281.

[16] Chen S J, Dill K A. RNA folding energy landscapes [J]. *Proc Natl Acad Sci USA*, 2000, **18**, **97**(2): 646-651.

[17] Comolli L R, Smirnov I, Xu L, *et al*. A molecular switch underlies a human telomerase disease [J]. *Proc Natl Acad Sci USA*, 2002, **99**(26): 16998-17003.

[18] Theimer C A, Blois C A, Feigon J. Structure of the human telomerase RNA pseudoknot reveals conserved tertiary interactions essential for function [J]. *Molecular Cell*, 2005, **17**(5): 671-682.

[19] Brierley I, Digard P, Inglis S C. Characterization of an efficient coronavirus ribosomal frameshifting signal: requirement for an RNA pseudoknot [J]. *Cell*, 1989, **57**(4): 537-547.

[20] Brierley I, Pennell S, Gilbert R J. Viral RNA pseudoknots: Versatile motifs in gene expression and replication [J]. *Nature Reviews Microbiology*, 2007, **5**(8): 598-610.

[21] Somogyi P, Jenner A J, Brierley I, *et al*. Ribosomal pausing during translation of an RNA pseudoknot [J]. *Molecular and Cellular Biology*, 1993, **13**(11): 6931-6940.

[22] Giedroc D P, Theimer C A, Nixon P L. Structure, stability and function of RNA pseudoknots involved in stimulating ribosomal frameshifting [J]. *Journal of Molecular Biology*, 2000, **298**(2): 167-185.

[23] Plant E P, Jacobs K L, Harger J W, *et al*. The 9-A solution: How mRNA pseudoknots promote efficient programmed-1 ribosomal frameshifting [J]: *RNA*, 2003, **9**(2): 168-174.

[24] Staple D W, Butcher S E. Pseudoknots: RNA structures with diverse functions [J]. *PLoS Biol*, 2005, **3**(6): 956-959.

[25] Namy O, Moran S J, Stuart D I, *et al*. A mechanical explanation of RNA pseudoknot function in programmed ribosomal frameshifting [J]. *Nature*, 2006, **441**(7090): 244-247.

[26] Hansen T M, Reihani S N, Oddershede L B, *et al*. Correlation between mechanical strength of messenger RNA pseudoknots and ribosomal frameshifting[J]. *Proc Natl Acad Sci USA*, 2007, **104**(14): 5830-5835.

[27] Cao S, Chen S J. Predicting ribosomal frameshifting efficiency [J]. *Physical Biology*, 2008, **5**: 016002.

[28] Pennell S, Manktelow E, Flatt A, *et al*. The stimulatory RNA of the Visna-Maedi retrovirus ribosomal frameshifting signal is an unusual pseudoknot with an interstem element [J]. *RNA*, 2008, **14**(7): 1366-1377.

[29] Cornish P V, Hennig M, Giedroc D P. A loop 2 cytidine-stem 1 minor groove interaction as a positive determinant for pseudoknot-stimulated −1 ribosomal frameshifting [J]. *Proc Natl Acad Sci USA*, 2005, **102**(36): 12694-12699.

[30] Theimer C A, Blois C A, Feigon J. Structure of the human telomerase RNA pseudoknot reveals conserved tertiary interactions essential for function[J]. *Mol Cell*, 2005, **17**(5): 671-682.

[31] Chen G, Wen J D, Tinoco I T Jr. Single-molecule mechanical unfolding and folding of a pseudoknot in human telomerase RNA [J]. *RNA*, 2007, **13**: 2175-2188.

[32] Chen G, Chang K Y, Chou M Y, *et al*. Triplex structures in an RNA pseudoknot enhance mechanical stability and increase efficiency of −1 ribosomal frameshifting [J]. *Proc Natl Acad Sci USA*, 2009, **106**: 12706-12711.

[33] Kang H, Tinoco I Jr. A mutant RNA pseudoknot that

promotes ribosomal frameshifting in mouse mammary tumor virus [J]. *Nucleic Acids Research*, 1997, **25**(10): 1943-1949.

[34] Liu B, Mathews D H, Turner D H. RNA pseudoknots: folding and finding [J]. *F1000 Biology Reports*, 2010, **2**: 2-8.

[35] Kang H, Hines J V, Tinoco I Jr. Conformation of a Non-frameshifting RNA pseudoknot from mouse mammary tumor virus [J]. *J Mol Biol*, 1996, **259**: 135-147.

[36] Zhuang Z Y, Jaeger L, Shea J E. Probing the structural hierarchy and energy landscape of an RNA T-loop hairpin [J]. *Nucleic Acids Research*, 2007, **35**(20): 6995- 7002.

[37] Kale L R, Skeel M, Bhandarkar R, *et al*. NAMD2: greater scalability for parallel molecular dynamics [J]. *J Comp Phys*, 1999, **151**: 283-312.

[38] Yeh I C, Hummer G. Diffusion and electrophoretic mobility of single-stranded RNA from molecular dynamics simulations [J]. *Biophys J*, 2004, **86**(2): 681-689.

[39] Zhang D Q, Konecny R, Baker N A, *et al*. Electrostatic interaction between RNA and protein capsid in cowpea chlorotic mottle virus simulated by a coarse-grain RNA model and a Monte Carlo approach [J]. *Biopolymers*, 2004, **75**: 325-337.

[40] Yu Tao, Pan Chunxu, Sang Jianping, *et al*. Comparison in structural stability between chain A and B of CLC-ec1 exchanger by using MD simulation [C]//*Proceedings of* 2011 4*th International Conference on Biomedical Engineering and Informatics* (*BMEI*). New York: IEEE Press, 2011: 1825-1828.

[41] Evelyn M, Adam M, Alexander D, *et al*. CHARMM force field parameters for simulation of reactive intermediates in native and thio-substituted ribozymes [J]. *Journal of Computational Chemistry*, 2007, **28**(2): 495-507.

[42] Swarnalatha Y R, Fabrice L, Martin K. DNA polymorphism: A comparison of force fields for nucleic acids [J]. *Biophysical Journal*, 2003, **84**: 1421-1449.

[43] Gong Z, Zhao Y J, Xiao Y. RNA stability under different combinations of amber force fields and solvation models [J]. *Journal of Biomolecular Structure & Dynamics*, 2010, **28**: 431-441.

[44] Tan Z J, Chen S J. Salt contribution to RNA tertiary structure folding stability [J]. *Biophysical Journal*, 2011, **101**: 176-187.

[45] Tan Z J, Chen S J. Predicting ion binding properties for RNA tertiary structures [J]. *Biophysical Journal*, 2010, **99**: 1565-1576.

[46] Tan Z J, Chen S J. RNA helix stability in mixed Na^+/Mg^{2+} solution [J]. *Biophysical Journal*, 2007, **92**: 3615-3632.

[47] Rivas E, Eddy S R. A dynamic programming algorithm for RNA structure prediction including pseudoknots [J]. *J Mol Biol*, 1999, **285**: 2053-2068.

[48] Xia T, SantaLucia J Jr, Burkard M E, *et al*. Thermodynamic parameters for an expanded nearest-neighbor model for formation of RNA duplexes with Watson-Crick base pairs [J]. *Biochemistry*, 1998, **37**: 14719-14735.

[49] Zuker M, Stiegler P. Optimal computer folding of large RNA sequences using thermodynamics and auxiliary information [J]. *Nucleic Acids Research*, 1981, **9**: 133-148.

[50] Zuker M. Computer prediction of RNA structure: Methods in enzymology [J]. *Methods in Enzymology*, 1989, **180**: 262-288.

[51] Mathews D H, SabinaJ, Zuker M, *et al*. Expanded Sequence Dependence of Thermodynamic Parameters Improves Prediction of RNA Secondary Structure [J]. *J Mol Biol*, 1999, **288**: 911-940.

[52] Nixon P L, Theimer C A, Giedroc D P. Thermodynamics of stabilization of RNA pseudoknots by cobalt(III) hexaammine [J]. *Biopolymers*, 1999, **50**: 443-458.

□